Forms of Zinc Accumulated in the Hyperaccumulator *Arabidopsis halleri*[1]

Géraldine Sarret*, Pierre Saumitou-Laprade, Valérie Bert[2], Olivier Proux, Jean-Louis Hazemann, Agnès Traverse, Matthew A. Marcus, and Alain Manceau

Environmental Geochemistry Group, Laboratoire de Géophysique Interne et Tectonophysique, University of Grenoble and Centre National de la Recherche Scientifique (CNRS), Boite Postale 53, 38041 Grenoble cedex 9, France (G.S., A.M.); Laboratoire de Génétique et Evolution des Populations Végétales, Université de Lille1 and CNRS, Bât SN2, 59655 Villeneuve d'Ascq cedex, France (P.S.-L., V.B.); Laboratoire de Cristallographie, CNRS, 25 avenue des Martyrs, Boite Postale 166, 38042 Grenoble cedex 9, France (O.P., J.-L.H.); Laboratoire pour l'Utilisation du Rayonnement Electromagnétique, Bât 209D, Centre Universitaire, Boite Postale 34, 91898 Orsay cedex, France (A.T.); and Advanced Light Source (ALS), Berkeley Lab, MS 6–2100, Berkeley, California 94720 (M.A.M.)

The chemical forms of zinc (Zn) in the Zn-tolerant and hyperaccumulator *Arabidopsis halleri* and in the non-tolerant and nonaccumulator *Arabidopsis lyrata* subsp. *petraea* were determined at the molecular level by combining chemical analyses, extended x-ray absorption spectroscopy (EXAFS), synchrotron-based x-ray microfluorescence, and μEXAFS. Plants were grown in hydroponics with various Zn concentrations, and *A. halleri* specimens growing naturally in a contaminated site were also collected. Zn speciation in *A. halleri* was independent of the origin of the plants (contaminated or non-contaminated) and Zn exposure. In aerial parts, Zn was predominantly octahedrally coordinated and complexed to malate. A secondary organic species was identified in the bases of the trichomes, which contained elevated Zn concentrations, and in which Zn was tetrahedrally coordinated and complexed to carboxyl and/or hydroxyl functional groups. This species was detected thanks to the good resolution and sensitivity of synchrotron-based x-ray microfluorescence and μEXAFS. In the roots of *A. halleri* grown in hydroponics, Zn phosphate was the only species detected, and is believed to result from chemical precipitation on the root surface. In the roots of *A. halleri* grown on the contaminated soil, Zn was distributed in Zn malate, Zn citrate, and Zn phosphate. Zn phosphate was present in both the roots and aerial part of *A. lyrata* subsp. *petraea*. This study illustrates the complementarity of bulk and spatially resolved techniques, allowing the identification of: (a) the predominant chemical forms of the metal, and (b) the minor forms present in particular cells, both types of information being essential for a better understanding of the bioaccumulation processes.

Metal tolerant plants have the ability to survive and reproduce on soils containing high concentrations of metals in forms that are toxic or inimical to other plants (Macnair and Baker, 1994). Metal-hyperaccumulating plants have the additional property of storing large amounts of metals in their aerial parts, more than typically 10,000 $\mu g\ g^{-1}$ dry weight for zinc (Zn; Baker and Walker, 1990). This characteristic makes hyperaccumulators highly suitable for phytoremediation, a soft method in which plants are used for the cleanup of metal-polluted soils (Brooks, 1998; Baker et al., 2000). The genetics and the biochemical processes involved in metal uptake, transport, and storage by hyperaccumulating plants are still poorly understood, although this basic information is fundamental for the improvement of the technique (Van Der Lelie et al., 2001). Zn is one of the most important metal contaminant in industrialized countries (Nriagu and Pacyna, 1988), and numerous studies have been conducted on the species *Thalspi caerulescens* (Vazquez et al., 1992, 1994; Pollard and Baker, 1996; Lasat et al., 1998, 2000; Küpper et al., 1999; Salt et al., 1999; Frey et al., 2000; Assunçaõ et al., 2001) and, to a lesser extent, on *Arabidopsis halleri* (Macnair et al., 1999; Bert et al., 2000; Küpper et al., 2000; Zhao et al., 2000). This latter species is of particular interest because it is one of the closest relatives to Arabidopsis (Koch et al., 2001), whose genome is entirely sequenced (Meinke et al., 1998; Kaul et al., 2000). This information, together with the huge amount of literature available on Arabidopsis, should facilitate our understanding of metal tolerance and hyperaccumulation in *A. halleri*.

A. halleri is a pseudo-metallophyte, which means that it is found both in polluted and non-polluted areas. It is known as a Zn hyperaccumulator, but recent studies showed that it can also hyperaccumu-

[1] This work was supported by the CNRS, "Programme Environnement, Vie et Société" (grant no. 00N55) and by the Nord-Pas-de-Calais Region, "Programme de Recherches Concertées."

[2] Present address: Centre National de Recherche sur les Sites et Sols Pollués (CNRSSP), 930 Bd. Lahure, Boite Postale 537, 59505 Douai cedex, France.

* Corresponding author; e-mail gsarret@ujf-grenoble.fr; fax 33–4–76–82–81–01.

Article, publication date, and citation information can be found at www.plantphysiol.org/cgi/doi/10.1104/pp.007799.

late cadmium (Dahmani-Muller et al., 2000; Küpper et al., 2000; Bert et al., 2002). By analyzing F_2 progenies produced by interspecific crosses between *A. halleri* and the non-tolerant and non-hyperaccumulating *Arabidopsis lyrata* subsp. *petraea* (*A.l.*), Macnair et al. (1999) demonstrated that Zn tolerance and Zn hyperaccumulation are two genetically independent characters. Moreover, by comparing Zn tolerance and Zn hyperaccumulation abilities of several populations of *A. halleri* originating from contaminated and uncontaminated areas, Bert et al. (2000) showed that both characters are constitutive properties of the species, but that populations from uncontaminated sites are slightly less Zn tolerant but exhibit higher Zn accumulation rates than populations from contaminated sites.

Recent studies by scanning electron microscopy and energy-dispersive x-ray microanalysis documented the cellular distribution of Zn in the tissues of *A. halleri* grown in hydroponics (Küpper et al., 2000; Zhao et al., 2000). In the leaves, Zn was mostly sequestered in the base of the trichomes and in mesophyll cells. Trichomes are epidermal hairs present at the surface of plant leaves, and their function can be as diverse as the exudation of various molecules, the protection against the wind and sunlight, or the storage of metals (Rodriguez et al., 1983). The chemical form of Zn accumulated in the trichomes and in mesophyll cells of *A. halleri* was not determined. Another study on *A. halleri* grown in Zn-containing hydroponics showed a correlation between the concentration of Zn and the concentration of phosphorus (P) and citric and malic acids in the roots (Zhao et al., 2000). The Zn-P correlation was attributed to Zn phosphate precipitates at the root surface. No Zn correlation with P or organic acids was found in the leaves.

In hydroponic studies, the nutrient solution used is generally devoid of silicon because this element is not considered essential to plants (Epstein, 1999). However, some Zn-containing silicate aggregates were observed in the cytoplasm and in pinocytotic vesicles of *A. halleri* leaves grown on polluted soils, suggesting that Zn was transiently present as Zn silicate in the cytoplasm, before being translocated and stored in the vacuoles in an undetermined form (Neumann and zur-Nieden, 2001).

The aim of this study is to address several open questions concerning the mechanisms of Zn tolerance and hyperaccumulation in *A. halleri*. First, what are the accumulation forms of Zn in the roots and in the aerial parts of *A. halleri*, and are they specific to this species or common to a non-tolerant and non-hyperaccumulating Arabidopsis species such as *A.l.*? Second, within *A. halleri* species, do Zn accumulation forms depend on the origin of the plant (contaminated or non-contaminated)? Third, does the nature of the growing medium (soil versus hydroponics) and Zn concentration in the nutrient solution influence Zn speciation in the plant? To address these questions, two populations of *A. halleri*, one originating from a contaminated site (*A.h.*-C) and one from a non-contaminated site (*A.h.*-NC), as well as a non-tolerant and non-hyperaccumulating species, *A.l.* (Macnair et al., 1999), were grown in hydroponics at various Zn levels. In addition, natural specimens of *A. halleri* growing in a contaminated soil were collected. The chemical form of Zn in the roots and in the aerial parts of the plants was studied by Zn K-edge extended x-ray absorption fine structure spectroscopy (EXAFS) on powder samples, and results were interpreted in light of elemental and organic acids concentrations. The localization and speciation of Zn in the leaves of *A. halleri* was also investigated at the micron scale by synchrotron-based x-ray microfluorescence (μSXRF) and μEXAFS spectroscopy.

Table I. *Zn, P, malate, citrate, and oxalate concentrations in the roots (R) and in the aerial parts (AP) of the plants*

Values are means of three samples ± SD.

Plant	[Zn] Solution	Concentrations										
		Zn			P		Malate		Oxalate		Citrate	
		R	AP	T[a]	R	AP	R	AP	R	AP	R	AP
	μM	μmol g^{-1}										
Plants grown in hydroponics												
A.h.-C	250	218 ± 15	160 ± 1	0.7	469 ± 5	67 ± 2	2 ± 1	165 ± 24	5 ± 0	5 ± 0	22 ± 4	31 ± 5
	100	105 ± 15	62 ± 1	0.6	419 ± 57	74 ± 6	6 ± 1	144 ± 28	5 ± 0	16 ± 3	10 ± 1	19 ± 5
	10	17 ± 4	11 ± 2	0.6	181 ± 45	67 ± 12	6 ± 0	113 ± 6	4 ± 0	18 ± 9	28 ± 7	18 ± 1
A.h.-NC	250	218 ± 30	217 ± 19	1.0	551 ± 54	73 ± 7	5 ± 2	221 ± 35	5 ± 0	10 ± 3	9 ± 1	6 ± 0
	100	74 ± 13	80 ± 3	1.1	239 ± 47	56 ± 7	21 ± 6	111 ± 32	5 ± 1	8 ± 4	56 ± 10	16 ± 5
A.l.	10	46 ± 2	6 ± 0	0.1	292 ± 2	77 ± 3	10 ± 4	220 ± 22	0 ± 0	0 ± 0	9 ± 1	10 ± 1
Plant from the contaminated soil												
A.h.-C	–	112 ± 11	169 ± 8	1.5	70 ± 5	95 ± 2	36 ± 5	447 ± 26	6 ± 0	34 ± 7	138 ± 24	59 ± 6

[a]Transfer coefficient = $[Zn]_{aerial\ parts}/[Zn]_{roots}$.

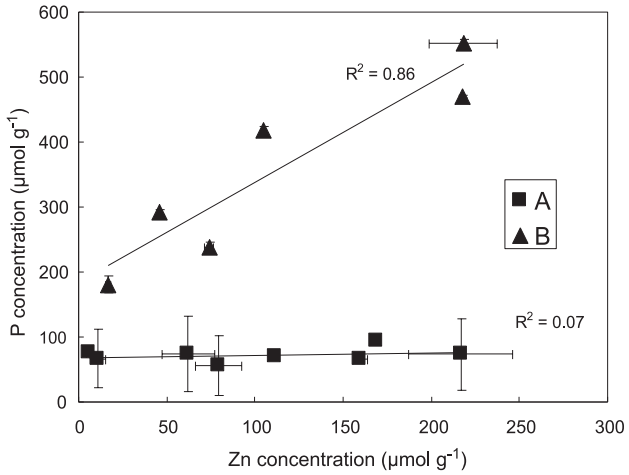

Figure 1. Relationship between Zn and P concentrations in the plant samples. Two groups of points can be defined: The first one (group A) represents the aerial parts of all plants and the roots of *A. halleri* from the contaminated soil. For these samples, Zn and P are not correlated (R^2, regression coefficient = 0.07). The second group (group B) represents the roots of all plants, except those of *A. halleri* from the contaminated soil. A Zn-P correlation clearly exists for these samples (R^2 = 0.86).

RESULTS

Elemental and Organic Acid Concentrations

Total concentrations of Zn, P, and organic acids in the aerial parts and in the roots of the plants are presented in Table I. For the two populations of *A. halleri* grown in hydroponics, Zn concentrations increased with Zn exposure. The transfer coefficient ($[Zn]_{aerial\ parts}/[Zn]_{roots}$) is always close to or less than 1, which is unexpected for a hyperaccumulating species. Such a low transfer coefficient was already observed in hydroponic experiments (Küpper et al., 2000), and is attributed to the precipitation of Zn phosphates on the root surface. Figure 1 shows that P and Zn concentration are clearly correlated in the roots of hydroponic plants (Fig. 1, group B), but not in the other samples (Fig. 1, group A, including the aerial parts of all plants and the roots of *A. halleri* grown on a contaminated soil). Moreover, *A. halleri* grown on a contaminated soil presents a higher transfer coefficient than hydroponic plants (1.5), which is consistent with a chemical precipitation of Zn phosphate on hydroponic roots only. This interpretation is also supported by EXAFS results (see below).

For a given Zn concentration in solution (250 or 100 μM Zn), the population from *A.h.*-NC accumulates more Zn in its aerial parts than that from *A.h.*-C, which confirms previous observations made at lower Zn concentration (50 μM; Bert et al., 2000). The higher aerial Zn accumulation in *A.h.*-NC was not accompanied by visible toxicity signs, such as chlorosis or low growth. *A.l.* grown in 10 μM Zn exhibits a very low transfer coefficient (0.1), as expected for a non-hyperaccumulating species.

The concentrations of the three organic acids most often inferred to bind metals (citrate, malate, and oxalate; Verkleij and Schat, 1989; Streit and Stumm, 1993; Brooks, 1998) were also measured, and compared with total Zn concentrations (Table I). In the roots, for all but two samples, the organic acid/Zn molar ratios were lower than 1 (Table I; Fig. 2). Moreover, the sum of the three organic acids/Zn ratio is lower than 1 for all but three samples. Thus, these ligands are not concentrated enough to bind all Zn atoms present in the roots. In the aerial parts, the malate to Zn molar ratio is higher than 1 in all the samples, whereas citrate to Zn and oxalate to Zn ratios are lower than 1. Thus, malate could bind all Zn atoms present in the aerial parts by forming 1:1 complexes (the predominant complex if we consider a solution containing equivalent concentrations of Zn and malate at pH 5.5, which is the pH of the vacuoles), whereas citrate and oxalate could not. However, the malate concentration is not linearly correlated to Zn (Fig. 2). These results differ from those obtained by Zhao et al. (2000) on *A. halleri* plants grown in hydroponics, in which malate and citrate were correlated to Zn in the roots, but not in the aerial parts.

Zn Speciation in the Bulk Samples

The Zn K-edge EXAFS spectra for all plant samples are shown in Figure 3. The whole set of data was first

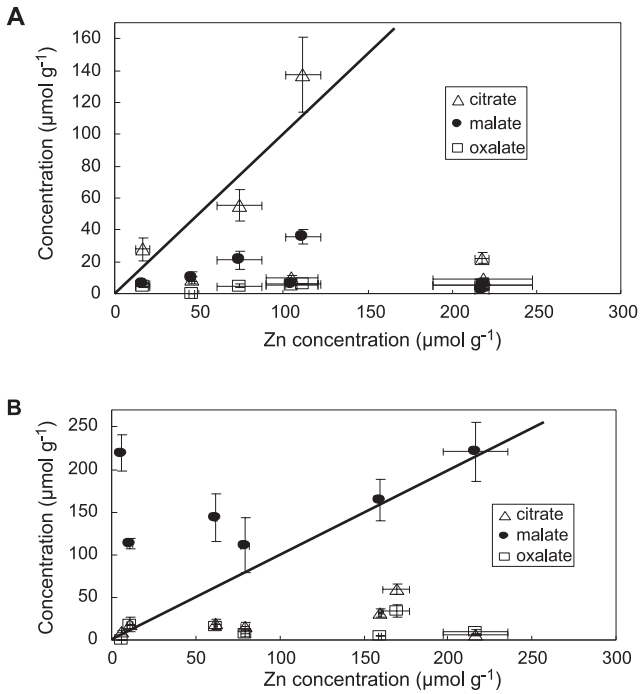

Figure 2. Organic acid content as a function of Zn content in the roots (A) and in the aerial parts (B) of the plants (values given in Table I). The line $y = x$ is shown in each plot.

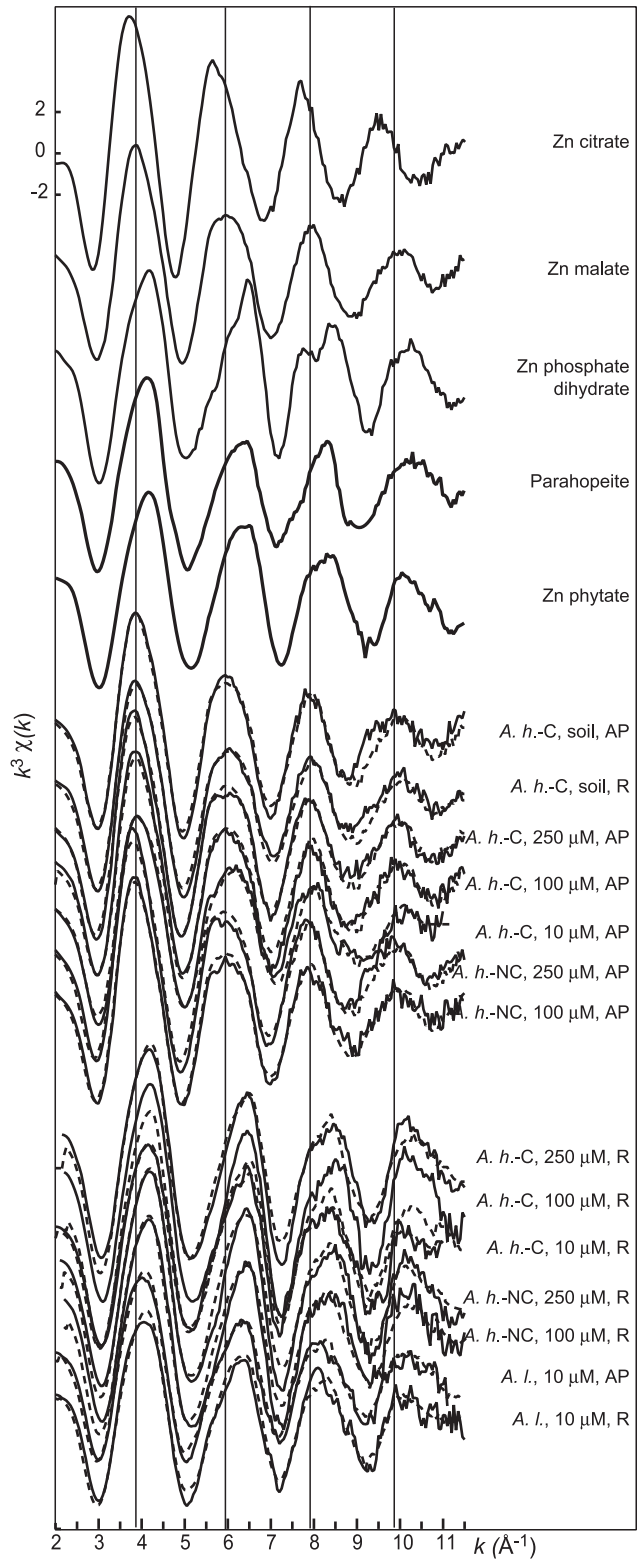

Figure 3. Zn K-edge EXAFS spectra for the plant samples (*A.h.*-C; *A.h.*-NC; *A.l.*; R, roots; AP, aerial parts) and for some Zn reference compounds. Solid lines are data and dashed lines are linear combinations of Zn malate and Zn phytate.

treated by principal component analysis (PCA; Ressler et al., 2000, and refs. therein). This statistical analysis allows the determination of the number of independent components contained in a set of spectra. The number of primary components corresponds to the number of Zn species present in the set of spectra, provided no species has a constant fractional amount ("background" species; Manceau et al., 2003). Then, an operation called "target transform" evaluates whether a reference spectrum is a likely principal component of the system. Once all components have been identified, their proportion in the various samples is determined by least square fitting of the unknown spectra to the combination of reference spectra previously identified by PCA. This approach is particularly powerful for the analysis of natural samples containing multiple forms of the same metal because the number and nature of these forms cannot be assumed a priori (Isaure et al., 2002). An important condition for the PCA is that the number of spectra should be greater than the number of unknown species, a condition amply satisfied here.

The number of primary components was evaluated from three criteria: the weight of each component, which is directly related to how much of the signal it represents, the indicator of each component, which reaches a minimum for the least significant component representing real signal (Malinowski, 1991), and the residuals between experimental and reconstructed spectra using one, two, three, or more components. If the system contains two principal components, each spectrum should be well fitted by two components, and adding a third one should not significantly improve the quality of the fit.

In the present study, the weights of the first four components were, in decreasing order, 107, 44, 8, and 6, with indicator values of 0.11, 0.04, 0.05, and 0.06, respectively. The spectra were correctly reconstructed with two components, with the normalized sum-square ($NSS = \Sigma[k^3\chi(k)_{exp} - k^3\chi(k)_{reconstr.}]^2 / \Sigma[k^3\chi(k)_{exp}]^2$) between 3.7×10^{-2} and 4.2×10^{-3}, and the quality of the fits was not much improved with three components (*NSS* between 2.5×10^{-2} and 3.5×10^{-3}). Thus, it was concluded from this analysis that two Zn species are significantly present in the set of samples. Note that species representing less than 10% of total Zn are not detected by this method.

The two statistically significant Zn species were subsequently identified by target transformation using a large library of reference spectra (aqueous Zn^{2+}, Zn complexed to organic acids and to amino acids, Zn sorbed on mineral surfaces, and Zn minerals; Sarret et al., 1998a; Manceau et al., 2000). Several references gave satisfactory fits, including Zn malate, Zn His, aqueous Zn^{2+}, Zn citrate, and Zn phytate. Other references, for instance Zn phosphate tetrahydrate or Zn oxalate, gave unsatisfactory fits. Among the five compounds retained, the most likely pair of primary components should allow the reproduction

Table II. *Proportion and amount of Zn malate and Zn phosphate species in the plant samples*

Sample	$[Zn]_{sol.}$	[Zn]	EXAFS						Chemical Analyses		
			Proportion of Zn species[a]				Concentrations[b]		Concentrations		
			Zn Malate		Zn Phosphate	NSS $\times 10^{-2}$[c]	Zn Malate	Zn Phosphate	Malate		P
	μM	$\mu mol\ g^{-1}$	*molar % of total Zn*				$\mu mol\ g^{-1}$		$\mu mol\ g^{-1}$		
Aerial parts											
A.h.-C	250	160 ± 1	100 ± 10		0 ± 10	2.5	160 ± 17	0 ± 16	165 ± 24		67 ± 2
	100	62 ± 1	100 ± 10		0 ± 10	4.1	62 ± 7	0 ± 6	144 ± 28		74 ± 6
	10	11 ± 2	67 ± 10		33 ± 10	5.6	7 ± 3	4 ± 2	113 ± 6		67 ± 12
A.h.-NC	250	217 ± 19	100 ± 10		0 ± 10	5.9	217 ± 43	0 ± 24	221 ± 35		73 ± 7
	100	80 ± 3	100 ± 10		0 ± 10	3.3	80 ± 11	0 ± 8	111 ± 32		56 ± 7
A.l.	10	6 ± 0	0 ± 10		100 ± 10	13.4	0 ± 1	6 ± 1	220 ± 22		77 ± 3
A.h.-C (soil)	–	169 ± 8	100 ± 10		0 ± 10	3.9	169 ± 26	0 ± 18	447 ± 26		95 ± 2
Roots											
A.h.-C	250	218 ± 15	0 ± 10		100 ± 10	9.4	0 ± 23	218 ± 38	2 ± 1		469 ± 5
	100	105 ± 15	0 ± 10		100 ± 10	14.8	0 ± 12	105 ± 27	6 ± 1		419 ± 57
	10	17 ± 4	0 ± 10		100 ± 10	9.4	0 ± 2	17 ± 6	6 ± 0		181 ± 45
A.h.-NC	250	218 ± 30	0 ± 10		100 ± 10	7.4	0 ± 25	218 ± 55	5 ± 2		551 ± 54
	100	74 ± 13	0 ± 10		100 ± 10	10.9	0 ± 9	74 ± 22	21 ± 6		239 ± 47
A.l.	10	46 ± 2	0 ± 10		100 ± 10	10.3	0 ± 5	46 ± 7	10 ± 4		292 ± 2
A.h.-C (soil)[d]	–	112 ± 11	75 ± 10		25 ± 10	3.6	84 ± 21	28 ± 15	36 ± 5		70 ± 5
			Zn Malate	Zn Citrate	Zn Phosphate		Zn Malate	Zn Citrate Zn Phosphate	Malate	Citrate	P
			29 ± 10	39 ± 10	32 ± 10	5.3	33 ± 15	44 35 ± 16	36 ± 5	138 ± 24	70 ± 5

[a]Proportions of Zn species (in molar % of total Zn) were determined by simulating the plant EXAFS spectra by a linear combination of Zn malate and Zn phytate spectra (Fig. 3). [b]Concentrations are calculated from the proportion of the two species and the total Zn concentrations (Table I). [c]The quality of the fit is estimated by: $NSS = \Sigma [k^3 \chi(k)_{exp} - k^3 \chi(k)_{reconstr.}]^2 / \Sigma [k^3 \chi(k)_{exp}]^2$. [d]For this sample, two Zn distributions are given, one including Zn malate and Zn phytate, and one including Zn citrate as well. The error bars correspond to an uncertainty of 10% for the proportion of Zn species, to the SD over three samples for the measured concentrations, and to the combination of both uncertainties for the deduced concentrations of Zn species.

of all the plant spectra by linear combinations of these two spectra. Thus, all possible pairs were tested, and Zn malate + Zn phytate was the only one satisfying this condition. Phytate, a *myo*-inositol *kis*-hexaphosphate, contains six phosphate groups, which lend the molecule a high affinity for cations (Cosgrove, 1980). In Zn phytate, the metal is 4-fold coordinated (R = 1.96 Å), with a second shell modeled by only one P atom at 3.08 Å, which corresponds to a disordered Zn phosphate environment. It is difficult to conclude on the presence of Zn phytate or disordered Zn phosphate mineral in the plant samples, so in the following text and in Table II, the generic term "Zn phosphate" will be used for this species. In this case study, the identification of the two species was facilitated by the fact that some samples were pure end members, i.e. contained 100% Zn malate or 100% Zn phosphate (Table II).

The percentage of Zn malate and Zn phosphate in each sample was estimated next by least square fitting the unknown spectra with linear combinations of the two references (Table II; Figs. 3 and 4). The fits pointed to Zn malate as the major species in the aerial parts of the two *A. halleri* populations and in the roots of *A. halleri* from the contaminated soil. These results are consistent with malate to Zn ratios (higher than 1) except for the roots of *A. halleri* grown on soil (Table II). In this latter sample, citrate is well represented (138 μmol g^{-1}). The simulation of the EXAFS spectrum by a mixture of Zn malate (29% ± 10%), Zn citrate (39% ± 10%), and Zn phytate (32% ± 10%) gave a satisfactory fit, with an *NSS* of 5.3×10^{-2}. Because Zn citrate was among the compounds positively identified by the target transformation, its presence in this sample is likely. The occurrence of Zn citrate in the other samples was tested by including Zn citrate as a third component of the simulations, but the proportions determined were always below 5%, which is within the precision of the method. The fact that the PCA pointed out two instead of three principal components may be because of the fact that Zn citrate is present in only one sample, in which it represents less than 50% of total Zn.

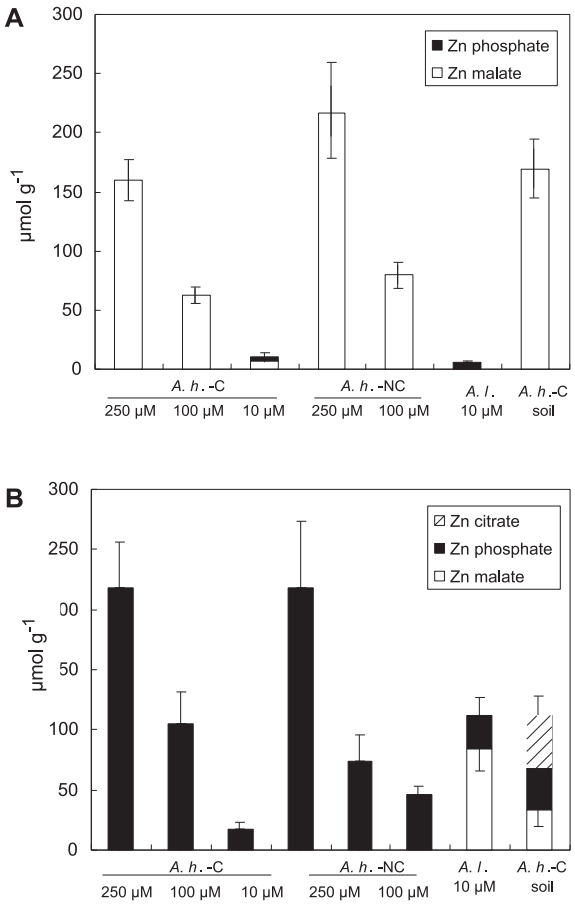

Figure 4. Concentration of Zn species in the aerial parts (A) and in the roots (B) of the plants calculated from EXAFS fitting percentages and Zn concentrations, as explained in Table II.

The leaves of *A.h.*-C exposed to 10 μM Zn contained Zn malate plus a minor proportion (33% ± 10% of total Zn, i.e. 4 μmol g^{-1}) of Zn phosphate. The fact that this Zn species was undetected at higher Zn concentration indicates that its proportion decreases when Zn increases (Fig. 4A). Zn phosphate was clearly the major Zn species in the roots of all plants grown in hydroponics, and in the aerial parts of *A.l.*

Zn structural parameters determined by numerical fits confirmed the results obtained by PCA and linear combinations (Table III; Fig. 5). In the aerial parts of all *A. halleri* plants, Zn was found to be octahedrally coordinated [d(Zn − O) = 1.99 to 2.03 Å] and surrounded by a next nearest C shell at 2.80 to 2.87 Å, in agreement with a Zn malate complex (Table III). In the roots of the hydroponic plants, and in the aerial parts of *A.l.*, the Zn-O distance [d(Zn − O) = 1.95 to 1.99 Å] is characteristic of a tetrahedral coordination, and the next nearest shell consists of P atoms at 3.06 to 3.16 Å as in phosphate compounds. Samples containing several Zn species (roots of *A.h.*-C grown on soil and aerial parts of *A.h.*-C grown in the 10 μM solution) have Zn structural parameters intermediate between those of the two (Zn malate and Zn phytate) or three (Zn malate, Zn citrate, and Zn phytate) references.

Zn Speciation in the Trichomes of *A. halleri*

High Zn concentrations were recently observed in the bases of the trichomes in the leaves of *A. halleri* (Küpper et al., 2000; Zhao et al., 2000). The distribution and speciation of Zn in the leaves of *A.h.*-C grown on the contaminated soil were investigated at the micron scale using μSXRF and Zn K-edge μEXAFS spectroscopy. Elemental maps of Ca and various metals present in the leaves are presented in Figure 6. Ca was almost evenly distributed in the leaf, whereas transition metals were concentrated in the bases of the trichomes. For instance, Zn signal

Table III. *Zn structural parameters in reference compounds and plant samples*

Structural parameters were obtained by simulating the first two coordination shells of Zn. *R*, Interatomic distance (Å); σ^2, Debye-Waller disorder factor (Å^2).

Sample		First Shell (O)			Atom	Second Shell			*Res*[a]
		N	*R*	σ^2		*N*	*R*	σ^2	
			Å	Å^2			Å	Å^2	
Reference compounds									
Zn Phytate		3.9	1.96	0.008	P	1.0	3.08	0.010	16
Zn malate		4.2	2.01	0.010	C	1.9	2.80	0.012	14
Zn citrate		4.3	2.03	0.010	C	3.5	2.76	0.012	12
Plant samples									
Aerial parts	$[Zn]_{solution}$ (μM)								
A.h.-C	250	4.5	2.01	0.010	C	1.9	2.87	0.009	16
	100	4.3	2.01	0.010	C	1.5	2.81	0.012	16
	10	3.7	1.99	0.009	C	2.0	2.86	0.010	24
A.h.-NC	250	4.5	2.03	0.010	C	2.1	2.80	0.012	17
	100	4.3	2.01	0.010	C	1.9	2.84	0.010	15
A.l.	10	4.1	1.99	0.010	P	1.3	3.07	0.011	17
A.h.-C (soil)	–	4.6	2.01	0.010	C	0.6	2.80	0.012	17
Roots									
A.h.-C	250	4.1	1.96	0.007	P	1.3	3.09	0.008	15
	100	4.3	1.95	0.007	P	1.5	3.09	0.009	15
	10	4.3	1.97	0.009					11
A.h.-NC	250	4.2	1.96	0.007	P	1.1	3.10	0.007	15
	100	4.0	1.96	0.008	P	1.7	3.16	0.009	8
A.l.	10	4.0	1.98	0.009	P	1.2	3.06	0.011	14
A.h.-C (soil)	–	4.3	2.00	0.011	C	1.2	2.77	0.012	18

[a]The quality of the fit is estimated by the residual $Res = \Sigma\ k^3\chi(k)_{exp} - k^3\chi(k)_{fit} / \Sigma\ k^3\chi(k)_{exp}$ *100. Estimated errors on *R* and *N* are ± 0.01 Å and ± 10% for the first shell, and ± 0.03 Å and ± 20% for the second shell, respectively.

was about 10-fold greater in these spots than in the leaf itself (75,000 counts/s/I_0 [incident intensity] compared with 4,000–8,000 counts/s/I_0). Considering the thickness of the leaf and the trichome spots, it corresponds to a Zn concentration at least 100-fold higher. The same elemental distribution was observed in other leaves of different ages. Zn K-edge μEXAFS spectra in different Zn "hot spots" were recorded and found to be identical. Figure 7 compares the μEXAFS spectrum of a trichome with the EXAFS spectra of the roots and aerial parts of *A.h.*-C, together with a selection of Zn references. The trichome spectrum is clearly different from all the others: Its frequency matches that of the roots of *A.h.*-C grown in hydroponics, but the two spectra clearly have a distinct shape. The trichome spectrum was compared with a large number of Zn organic and mineral references (see previous paragraph), but no good match was obtained. The occurrence of mineral Zn in this highly metal-concentrated zone was ruled out because EXAFS spectra of inorganic compounds such as zincite or hydrozincite exhibit complex shapes because of the presence of heavy atoms in the second or higher coordination shells (Fig. 7). The comparison of the RDF for the trichome and the bulk plant samples indicates that Zn is tetrahedrally coordinated, as in the roots of the hydroponic plant (Fig. 8). The second shell peak of the trichome is centered at $R + \Delta R = 2.5$ Å, compared with 2.6 Å for the aerial parts (C shell) and 2.8 Å for the roots (P shell). This short distance is suggestive of a C shell (Sarret et al., 1998a). This structural interpretation is strongly supported by the relative position of the modulus and imaginary part of the Fourier transform, whose maxima are superimposed in the case of a Zn-P pair, and opposite for a Zn-C pairs (see arrows in Fig. 8; Sarret et al., 1998a). Hence, the second coordination shell of Zn in the trichome likely consists of C atoms.

These data suggest that in the bases of the trichomes, Zn is 4-fold coordinated and complexed to carboxyl and/or hydroxyl groups belonging to organic acid(s). This chemical form differs from the average form (i.e. Zn malate) identified by powder EXAFS, which means that it is quantitatively minor. Despite the high concentration of Zn in the base of the trichomes, these cells account for a minor proportion of the leaf biomass, so they do not represent the major sink of Zn. The combination of μEXAFS and powder EXAFS shows that the metal is distributed as Zn malate in the leaf itself (predominant form), and as a tetrahedral Zn-organic acid(s) complex in the trichomes (minor form).

DISCUSSION

A. halleri is supposed to accumulate Zn in the vacuolar compartment of the leaves (Neumann and zur-

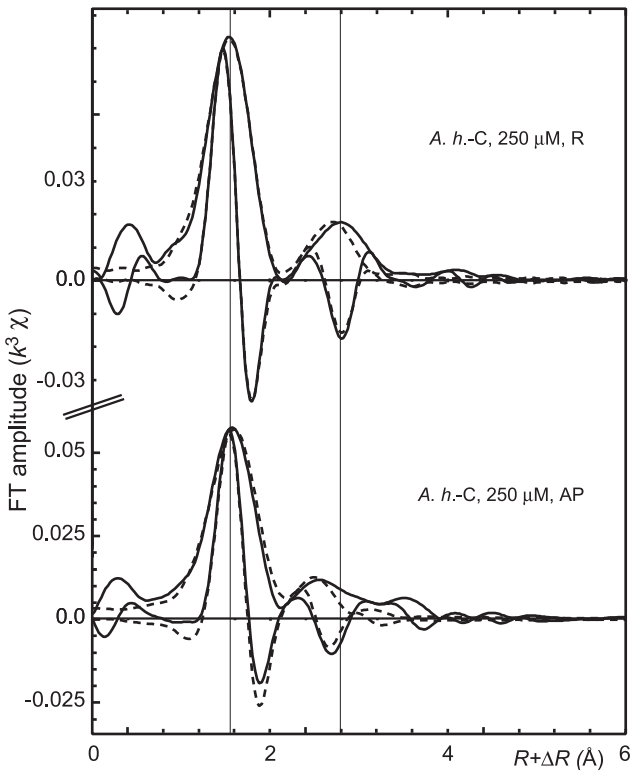

Figure 5. Radial distribution functions (RDFs; modulus and imaginary part) for the roots and the aerial parts of *A.h.*-C grown in solution containing 250 μM Zn. Solid lines are data and dashed lines are numerical simulations. EXAFS parameters are given in Table III.

Nieden, 2001), similar to *T. caerulescens* (Vazquez et al., 1992; Küpper et al., 1999; Frey et al., 2000). Organic acids, including malate, citrate, and oxalate, are primarily located in the vacuoles (Ryan and Walker-Simmons, 1983); thus, are often inferred to chelate metals. In *T. caerulescens*, malate was shown to be the most abundant organic acid in the shoots (164–248 μmol g^{-1} fresh weight), followed by citrate, succinate, and oxalate (Tolra et al., 1996). However, x-ray absorption near edge structure spectroscopy showed that malate was not involved in Zn binding in this species, the chemical forms of Zn being, in decreasing proportion, citrate, aqueous Zn^{2+}, His, and Zn bound to the cell wall (Salt et al., 1999). In the present study, EXAFS and chemical analyses showed that Zn is predominantly complexed to malate in the leaves of the two *A. halleri* populations. A secondary Zn organic species was identified in the trichomes, in which Zn is tetrahedrally coordinated and complexed to carboxyl and/or hydroxyl functional groups. The function of the trichomes in metal storage or exudation is still unclear.

Although *A.l.* has a malate to Zn molar ratio much higher than 1 in its aerial parts, this non-tolerant and non-hyperaccumulating species sequesters Zn as a phosphate species, similar to various crop species (Van Steveninck et al., 1994; Sarret et al., 2001). The fact that malate is not a marker of tolerance and hyperaccumulation is also supported by the results of Shen et al. (1997), who showed that the hyperaccumulator *T. caerulescens* and the non-tolerant and non-hyperaccumulator *Thlaspi ochroleucum* had constitutively high concentrations of malate in shoots. Instead, the location of malate (vacuolar or cytoplasmic) and the quantity of Zn transmembrane transporters (Lasat et al., 2000; Pence et al., 2000; Assunçaõ et al., 2001) are probably key factors conditioning Zn hyperaccumulation.

In the roots of hydroponic plants, Zn was speciated as inorganic or organic Zn phosphate. Because phosphate precipitates have been observed previously at the root surface of hydroponic plants (Küpper et al., 2000; Zhao et al., 2000), the inorganic form is more likely. Although the nutrient solutions were undersaturated with respect to Zn-phosphate solids, chemical precipitation may have been induced by the root activity. This phenomenon would account for the low measured values of the root-to-leaf transfer coefficients (Table I). Zn phosphate was also present in small proportion in the roots of the plant grown on soil. Its location, either at the surface of the roots or inside the cells, is unknown, but the high P content of the soil (3–4 g kg^{-1} dry weight P_2O_5) tends to favor the first hypothesis.

These results were obtained on freeze-dried and ground plant materials for bulk EXAFS experiments, and on freeze-dried whole leaves for μEXAFS experiments. For bulk EXAFS, grinding is required to obtain homogeneous samples at the scale of the x-ray beam (a few hundred micrometers in our experiment). To avoid chemical reactions between different cell compartments during this step, the plant material can be frozen or freeze dried. This latter conditioning was preferred to avoid a possible partial defrosting and mixing of the cell compartments during grinding or sample transfer. However, it is difficult to completely dismiss the possibility of artifacts induced by this preparation. For instance, could Zn malate and Zn phosphate be the products of reactions occurring during the dehydration between Zn^{2+}, malate, and phosphate ions? The high affinity of Zn^{2+} for malate and phosphate (complexation constant log $K = 2.9$ for Zn malate, Smith and Martell, 1982; solubility constant log $K_s = -32$ for Zn phosphate tetrahydrate, MINTEQA2 database) is a point in favor of the preexistence of the two species in the fresh material. Moreover, these reactions would imply proton exchange, whose possible occurrence at low temperature (−52°C in the freeze dryer used in this work) is unknown to our knowledge.

In conclusion, the major, and some minor, chemical forms of Zn in the aerial parts and in the roots of *A. halleri* and *A.l.* have been elucidated at the molecular scale by the combination of chemical analyses and EXAFS spectroscopy. However, the role of the genes involved in Zn tolerance and hyperaccumulation on the speciation of Zn is still unknown. In addition, the

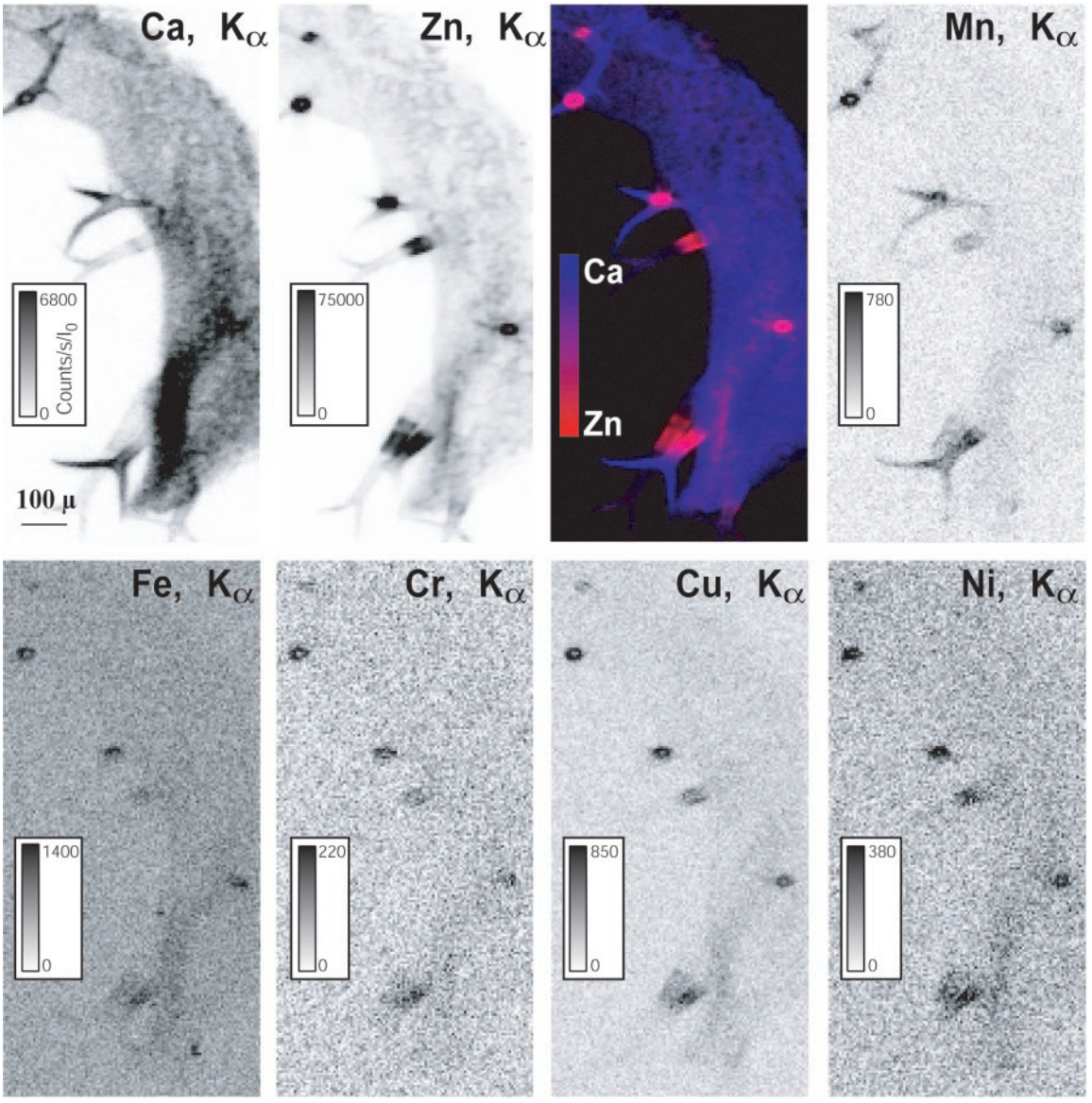

Figure 6. μSXRF elemental maps of a leaf fragment (incident beam energy, 9.7 KeV; beam size and pixel size, 5 × 5 μm; dwell time, 150 ms pixel^{-1}). The number of fluorescence yield counts were normalized by I_0 and the dwell time. Metals are concentrated in the bases of the trichomes.

biochemical processes responsible for Zn absorption, transfer, and storage remain to be clearly delineated.

MATERIALS AND METHODS

Plant Origins

Seeds of *Arabidopsis halleri* were collected on single mother plants in 1999 at two different sites. Seeds of *A. halleri* from the polluted site (*A.h.*-C) were collected in a field contaminated by the atmospheric fallouts of a nearby Zn smelter in Auby (North of France). *A.h.*-NC seeds were collected in Tatransla Javorina, a conservation area of the High Tatras in Slovakia. *Arabidopsis lyrata* subsp. *petraea* (*A.l.*) originated from Unhošt, a non-contaminated woodland in the valley of Lodenice in Central Bohemia (Czech Republic).

Plant Culture

Seeds were germinated on sand in a greenhouse, and 8 weeks after germination, seedlings were transferred to 10-L polycarbonate vessels (six plants per vessel) containing a growth medium. The medium consisted of 0.5 mM $Ca(NO_3)_2$, 0.2 mM $MgSO_4$, 0.5 mM KNO_3, 0.1 mM K_2HPO_4, 0.2 μM $CuSO_4$, 2 μM $MnCl_2$, 10 μM H_3BO_3, 0.1 μM MoO_3, 10 μM FeEDDHA, and 0.2 μM $ZnSO_4$. The vessels were kept in a controlled growth chamber (temperature, 20°C day/15°C night; light, 16-h day/8-h night). The pH of the solution was maintained at 5.0 ± 0.1 using MES acid buffer (2 mM), which is known to be chemically inert toward metals. After 3 weeks, the nutrient solutions received $ZnSO_4$ at the following concentrations: 10, 100, or 250 μM for *A.h.*-C; 100 or 250 μM for *A.h.*-NC (the plants grown on 10 μM were accidentally lost); and 10 μM for *A.l.* (one vessel containing six plants per Zn concentration). The theoretical speciation of Zn in the nutrient solutions was calculated using the MINTEQA2 program. Zn speciation was almost constant at the three Zn concentrations, with free Zn^{2+} as major species (84%–85%), and aqueous $ZnSO_4$ as minor species (15%–16%). The saturation

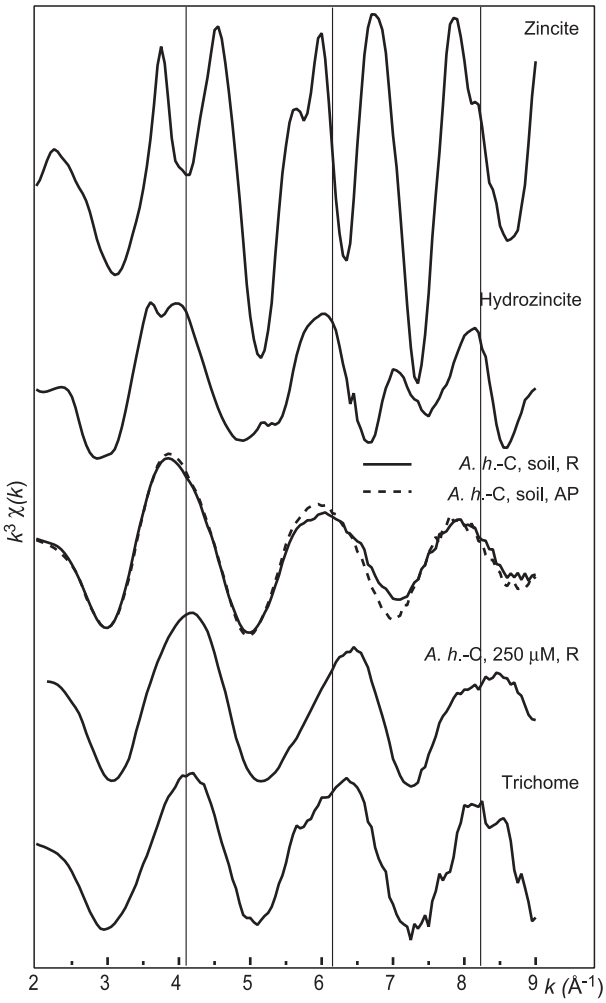

Figure 7. Comparison of the μEXAFS spectrum for the trichome with the powder EXAFS spectra for *A.h.*-C and for a selection of reference compounds.

indexes for Zn minerals were always negative, so no Zn precipitates should have formed. During the experiment, nutrient solutions were renewed every 8 d. The position under lights in the growth chamber was randomly modified each 4 d. Plants were harvested after 5 weeks of Zn treatment. In parallel to the hydroponic culture, six *A. halleri* plants growing naturally in the polluted site of Auby were sampled. After harvesting, plant samples were rinsed with deionized water and divided into roots and aerial parts. For each species and each culture condition, the roots and the aerial parts of the six plants were pooled to have enough material for the EXAFS and chemical analyses and freeze dried. To allow a rapid freezing, each sample was placed in a large container, transferred into the freeze dryer at room temperature, and the container was filled with liquid nitrogen before starting the dehydration. The samples were then ground using a mechanical agate mill. An aliquot was kept for EXAFS, and the rest was divided into six aliquots, three for the analysis of Zn and P, and three for the analysis of organic acids. Some freeze-dried leaves of *A. halleri* from the contaminated site were kept for μSXRF and μEXAFS analysis.

Chemical Analyses

For Zn and P analysis, plant powders were digested with $HNO_3/HClO_4$ (80:20 [v/v]) and Zn and P concentrations were determined using inductively coupled atomic emission spectrometry. For the determination of malic, citric, and oxalic acid concentrations, the plant powders were placed in a 0.1 N HCl solution and ultrasonicated for 1 h to extract and dissociate the Zn-organic acids complexes. The suspension was then filtered at 0.45 μm, and cations were extracted from the solution using a cationic exchange resin (On Guard H, Dionex, Sunnyvale, CA). The solution was then neutralized to pH 7 using a 1 N NaOH solution. Organic acids concentrations were measured by ionic chromatography (Dionex DX500). All values are given as mean concentrations over three samples ± SD.

X-Ray Absorption Spectroscopy

Zn malate standard was obtained by slow evaporation of a solution containing 10^{-2} M $Zn(NO_3)_2$ and 8×10^{-2} M Na malate at pH 5.5. Zn citrate was purchased from Alfa (Berkshire, UK). Zn phytate was kindly provided by J. Cotter-Howells (University of Aberdeen, Scotland). Other Zn standards were presented previously (Sarret et al., 1998a, 1998b; Manceau et al., 2000; Isaure et al., 2002). Pressed pellets were prepared from the aerial parts and roots powder. Zn K-edge EXAFS spectra of Zn-rich samples were measured at room temperature on beam line D42 at the Laboratoire du Rayonnement Electromagnétique (Orsay, France) in transmission mode using ionization chambers, and on beam line BM32 at the European Synchrotron Radiation Facility (Grenoble, France) in fluorescence mode using a 30-element solid-state Ge detector (St. Quentin Yvelines, France) for diluted samples ([Zn] < 5,000 mg kg^{-1}). Data extraction was performed according to standard methods. The PCA and the least square spectral decomposition were performed with our own software, and EXAFS structural parameters (coordination nos., interatomic distances, and Debye Waller factors) were determined using WinXAS 2.0 (Ressler, 1997). For this determination, k^3-weighted $\chi(k)$ functions were Fourier transformed over the 3.5- to 12-$Å^{-1}$

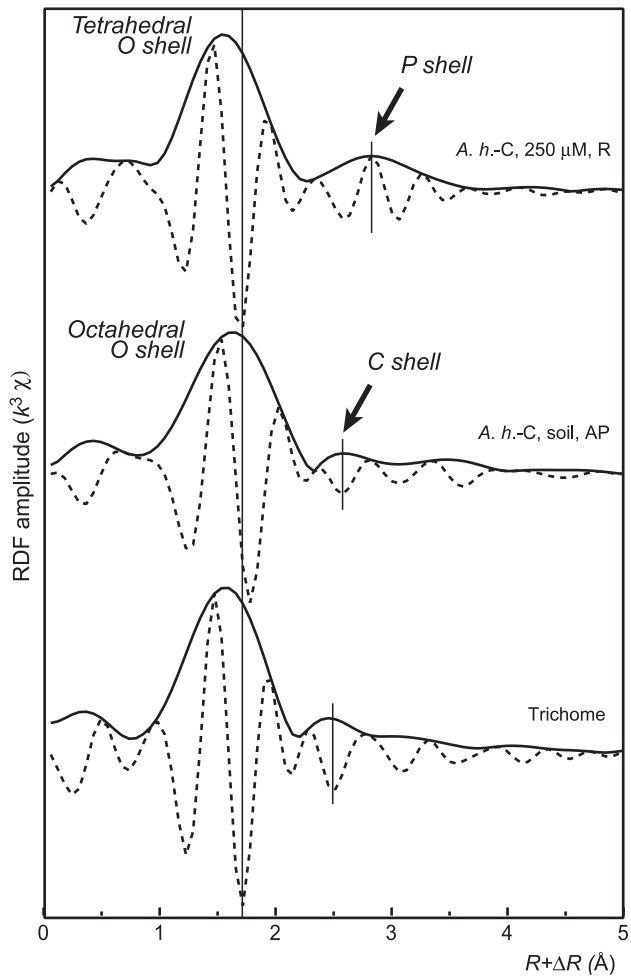

Figure 8. RDFs for the trichome and for powder samples (roots and aerial part) of *A.h.*-C.

range using a Bessel window with a smoothing parameter of 4. Then, fits of the first two shells were carried out using Zn-O, Zn-P, and Zn-C theoretical scattering functions calculated with FEFF7 (Rehr et al., 1991) from the structure of Zn malate dihydrate (Reed and Karipides, 1976) and hopeite (Whitaker, 1975). Fits were performed both in *k* and *R* space to check for consistency.

Microprobe Analyses

μSXRF and Zn K-edge μEXAFS measurements on the leaves of *A.h.*-C grown on the soil were performed on beam line 10.3.2 at the ALS (Berkeley, CA), operating at 1.9 GeV and 200 to 400 mA. Fragments of freeze-dried leaves were fixed on a kapton tape, mounted on an *x-y* translation stage, and studied in air at room temperature. The beam was focused using a pair of elliptically bent mirrors in the Kirkpatrick-Baez configuration (Kirkpatrick and Baez, 1948). The incident beam intensity was measured using two copper paddles forming a miniature ionization chamber, and the fluorescence yield was measured using a seven-element Ge solid-state detector. For μSXRF, the spot size was 5×5 μm, and the fluorescence yield was normalized by I_0 and the dwell time. Four maps of different leaves were recorded. For μEXAFS, the spot size was 15×5 μm. Three μEXAFS scans were performed on a Zn-rich trichome from three different leaves. All spectra were identical.

ACKNOWLEDGMENTS

We would like to acknowledge the European Synchrotron Radiation Facility (Grenoble, France), the Laboratoire du Rayonnement Electromagnétique (Orsay, France), and the ALS (Berkeley, CA) for the provision of beam time. We are grateful to Vlastimil Mikolas for help in finding population sites in Slovakia, to Marc Macnair for providing seeds of *A.l.*, to Nicolas Geoffroy for his technical support, and to Jaco Vangronsveld for fruitful discussions.

Received April 30, 2002; returned for revision May 26, 2002; accepted July 17, 2002.

LITERATURE CITED

Assunçaõ AGL, Martins PD, De Folter S, Vooijs R, Schat H, Aarts MGM (2001) Elevated expression of metal transporter genes in three accessions of the metal hyperaccumulator *Thlaspi caerulescens*. Plant Cell Environ **24:** 217–226

Baker AJM, McGrath SP, Reeves RD, Smith JAC (2000) Metal hyperaccumulator plants: a review of the ecology and physiology of a biochemical resource for phytoremediation of metal-polluted soils. *In* N Terry, G Banuelos, J Vangronsveld, eds, Phytoremediation of Contaminated Soil and Water. Lewis Publishers, Boca Raton, FL, pp 85–107

Baker AJM, Walker PL (1990) Ecophysiology of metal uptake by tolerant plants. *In* AJ Shaw, ed, Heavy Metal Tolerance in Plants: Evolutionary Aspects. CRC Press, Boca Raton, FL, pp 155–177

Bert V, Bonnin I, Saumitou-Laprade P, de Laguérie P, Petit D (2002) Do *Arabidopsis halleri* from nonmetallicollous populations accumulate zinc and cadmium more effectively than those from metallicolous populations? New Phytol **155:** 47–57

Bert V, Macnair MR, De Laguerie P, Saumitou-Laprade P, Petit D (2000) Zinc tolerance and accumulation in metallicolous populations of *Arabidopsis halleri* (Brassicaceae). New Phytol **146:** 225–233

Brooks RR (1998) Plants That Hyperaccumulate Heavy Metals. CAB International, Wallingford, UK

Cosgrove DJ (1980) Inositol Phosphate. Their Chemistry, Biochemistry and Physiology. Elsevier, New York

Dahmani-Muller H, Van-Oort F, Gelie B, Balabane M (2000) Strategies of heavy metal uptake by three plant species growing near a metal smelter. Environ Pollut **109:** 231–238

Epstein E (1999) Silicon. Annual review of plant physiology. Plant Mol Biol **50:** 641–664

Frey B, Keller C, Zierold K, Schulin R (2000) Distribution of Zn in functionally different leaf epidermal cells of the hyperaccumulator *Thlaspi caerulescens*. Plant Cell Environ **23:** 675–687

Isaure MP, Laboudigue A, Manceau A, Sarret G, Tiffreau C, Trocellier P, Lamble G, Hazemann JL, Chateigner D (2002) Quantitative Zn speciation in a contaminated dredged sediment by μ-PIXE, μ-SXRF, EXAFS spectroscopy and principal component analysis. Geochim Cosmochim Acta **66:** 1549–1567

Kaul S, Koo HL, Jenkins J, Rizzo M, Rooney T, Tallon LJ, Feldblyum T, Nierman W, Benito MI, Lin XY et al. (2000) Analysis of the genome sequence of the flowering plant *Arabidopsis thaliana*. Nature **408:** 796–815

Kirkpatrick P, Baez AV (1948) Formation of optical images by X-rays. J Opt Soc Am **38:** 766

Koch M, Haubold B, Mitchell-Olds T (2001) Molecular systematics of the Brassicaceae: evidence from coding, plastidic *MatK* and nuclear *Chs* sequences. Am J Bot **88:** 534–544

Küpper H, Lombi E, Zhao FJ, McGrath SP (2000) Cellular compartmentation of cadmium and zinc in relation to other elements in the hyperaccumulator *Arabidopsis halleri*. Planta **212:** 75–84

Küpper H, Zhao FJ, McGrath SP (1999) Cellular compartmentation of zinc in leaves of the hyperaccumulator *Thlaspi caerulescens*. Plant Physiol **119:** 305–311

Lasat MM, Baker AJM, Kochian LV (1998) Altered Zn compartmentation in the root symplasm and stimulated Zn absorption into the leaf as mechanisms involved in Zn hyperaccumulation in *Thlaspi caerulescens*. Plant Physiol **118:** 875–883

Lasat MM, Pence NS, Garvin DF, Ebbs SD, Kochian LV (2000) Molecular physiology of zinc transport in the Zn hyperaccumulator *Thlaspi caerulescens*. J Exp Bot **51:** 71–79

Macnair MR, Baker AJM (1994) Metal tolerance in plants: evolutionary aspects. *In* ME Farago, ed, Plants and the Chemical Elements. VCH, Weinheim, Germany, pp 68–86

Macnair MR, Bert V, Huitson SB, Saumitou-Laprade P, Petit D (1999) Zinc tolerance and hyperaccumulation are genetically independent characters. Proc R Soc Lond B **266**: 2175–2179

Malinowski ER (1991) Factor Analysis in Chemistry. John Wiley, New York

Manceau A, Lanson B, Schlegel ML, Hargé JC, Musso M, Eybert-Bérard L, Hazemann JL, Chateigner D, Lamble GM (2000) Quantitative Zn speciation in smelter-contaminated soils by EXAFS spectroscopy. Am J Sci **300:** 289–343

Manceau A, Marcus MA, Tamura N (2003) Quantitative speciation of heavy metals in soils and sediments by synchrotron X-ray techniques. *In* NC Sturchio, P Fenter, SR Sutton, ML Rivers, eds, Applications of Synchrotron Radiation in Low-Temperature Geochemistry and Environmental Science. Reviews in Mineralogy. Mineralogical Society of America, Washington, D.C. (in press)

Meinke DW, Cherry JM, Dean C, Rounsley SD, Koornneef M (1998) *Arabidopsis thaliana*: a model plant for genome analysis. Science **282:** 662

Neumann D, zur-Nieden U (2001) Silicon and heavy metal tolerance of higher plants. Phytochemistry **56:** 685–692

Nriagu JO, Pacyna JM (1988) Quantitative assessment of worldwide contamination of air, water and soils by trace metals. Nature **333:** 134–139

Pence NS, Larsen PB, Ebbs SD, Letham DLD, Lasat MM, Garvin DF, Eide D, Kochian LV (2000) The molecular physiology of heavy metal transport in the Zn/Cd hyperaccumulator *Thlaspi caerulescens*. Proc Natl Acad Sci USA **97:** 4956–4960

Pollard AJ, Baker AJM (1996) The quantitative genetics of zinc hyperaccumulation in *Thlaspi caerulescens*. New Phytol **132:** 113–118

Reed AT, Karipides A (1976) The crystal structure of *S*-malatodiaquozinc(II) hydrate. Acta Cryst **B32:** 2085

Rehr JJ, Mustre de Leon J, Zabinsky SI, Albers RC (1991) Theoretical x-ray absorption fine structure standards. J Am Chem Soc **113:** 5135–5145

Ressler T (1997) WinXAS: a new software package not only for the analysis of energy-dispersive XAS data. J Physique IV **7**: c2–269

Ressler T, Wong J, Roos J, Smith IL (2000) Quantitative speciation of Mn-bearing particulates emitted from autos burning (methylcyclopentadienyl) manganese tricarbonyl-added gasolines using XANES spectroscopy. Environ Sci Technol **34:** 950–958

Rodriguez E, Healey PL, Mehta I (1983) Biology and Chemistry of Plant Trichomes. Plenum Press, New York

Ryan CA, Walker-Simmons M (1983) Plant vacuoles. Methods Enzymol **96:** 580–589

Salt DE, Prince RC, Baker AM, Raskin I, Pickering IJ (1999) Zinc ligands in the metal hyperaccumulator *Thlaspi caerulescens* as determined using X-ray absorption spectroscopy. Environ Sci Technol **33:** 713–717

Sarret G, Manceau A, Spadini L, Roux JC, Hazemann JL, Soldo Y, Eybert-Bérard L, Menthonnex JJ (1998a) Structural determination of Zn and Pb binding sites in *Penicillium chrysogenum* cell walls by EXAFS spectroscopy. Environ Sci Technol **32:** 1648–1655

Sarret G, Manceau A, Cuny D, Van Haluwyn C, Deruelle S, Hazemann JL, Soldo Y, Eybert-Bérard L, Menthonnex JJ (1998b) Mechanism of lichen resistance to metallic pollution. Environ Sci Technol **32:** 3325–3330

Sarret G, Vangronsveld J, Manceau A, Musso M, D'Haen J, Menthonnex JJ, Hazemann JL (2001) Accumulation forms of Zn and Pb in *Phaseolus vulgaris* in the presence and absence of EDTA. Environ Sci Technol **35:** 2854–2859

Shen ZG, Zhao FJ, McGrath SP (1997) Uptake and transport of zinc in the hyperaccumulator *Thlaspi caerulescens* and the non-hyperaccumulator *Thlaspi ochroleucum*. Plant Cell Environ **20:** 898–906

Smith RM, Martell AE (1982) Critical Stability Constants, Vol 3. Plenum Press, New York, p 126

Streit B, Stumm W (1993) Chemical properties of metals and the process of bioaccumulation in terrestrial plants. *In* B Markert, ed, Plants as Biomonitors. VCH, Weinheim, Germany, pp 29–62

Tolra RP, Poschenrieder C, Barcelo J (1996) Zinc hyperaccumulation in *Thlaspi caerulescens*: II. Influence on organic acids. J Plant Nutr **19:** 1541–1550

Van Der Lelie N, Schwitzguebel JP, Glass DJ, Vangronsveld J, Baker A (2001) Assessing phytoremediation's progress in the United States and Europe. Environ Sci Technol **35:** 446A–452A

Van Steveninck RFM, Barbare A, Fernando DR, Van Steveninck ME (1994) The binding of zinc, but not cadmium, by phytic acid in roots of crop plants. Plant Soil **167:** 157–164

Vazquez MD, Barcelo J, Poschenrieder C, Madico J, Hatton P, Baker AJM, Cope GH (1992) Localization of zinc and cadmium in *Thlaspi caerulescens* (Brassicaceae), a metallophyte that can hyperaccumulate both metals. J Plant Physiol **140:** 350–355

Vazquez MD, Poschenrieder C, Barcelo J, Baker AJM, Hatton P, Cope GH (1994) Compartmentation of zinc in roots and leaves of the zinc hyperaccumulator *Thlaspi caerulescens* J & C Prel. Bot Acta **107:** 243–250

Verkleij JAC, Schat H (1989) Mechanisms of metal tolerance in higher plants. *In* AJ Shaw, ed, Heavy Metal Tolerance in Plants: Evolutionary Aspects. CRC Press, Boca Raton, FL, pp 179–193

Whitaker A (1975) The crystal structure of hopeite, $Zn_3(PO_4)_2$, $4H_2O$. Acta Cryst **B31:** 2026–2035

Zhao FJ, Lombi E, Breedon T, McGrath SP (2000) Zinc hyperaccumulation and cellular distribution in *Arabidopsis halleri*. Plant Cell Environ **23:** 507–514